Sensors & Actuators: B. Chemical 402 (2024) 135075

Contents lists available at ScienceDirect

Sensors and Actuators: B. Chemical

journal homepage: www.elsevier.com/locate/snb

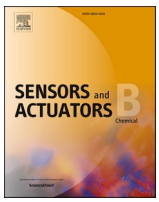

# A point-of-care single nucleotide variation assay based on strand-displacement-triggered recombinase polymerase amplification

Lutan Zhang [a,1], Lulu Xu [c,1], Jian Zhang [a], Wenbo Wang [a], Yanru Huang [a], Yixi Zhou [a], Xingmei Yao [a], Zhaohui Liu [b,*], Yunsheng Ge [a,*]

[a] Department of Central Laboratory, Women and Children's Hospital, School of Medicine, Xiamen University, Xiamen 361001, PR China
[b] The Graduate School of Fujian Medical University, Fuzhou 350001, PR China
[c] Department of Laboratory Medicine, Shandong Provincial Hospital Affiliated to Shandong First Medical University, Jinan 250000, PR China

ARTICLE INFO

*Keywords:*
Recombinase polymerase amplification (RPA)
Strand-displacement reaction (SDR)
Single nucleotide variation (SNV)
Codon 17 (A>T) mutation
Lateral flow assay
Point-of-care (POC) detection

ABSTRACT

The single nucleotide variation (SNV) assay holds significant value in the diagnosis of genetic diseases. However, the wide application of SNV analysis in clinics meets many difficulties because of the long test time and the limited experimental conditions. In this study, we develop a lateral flow-based strand-displacement-triggered recombinase polymerase amplification (SD-triggered RPA) assay for detecting β-thalassemia-related SNV (codon 17 (A>T) mutation), which is sensitive, fast, simple and easy to interpret in clinics. By innovatively integrating toehold-mediated strand displacement into recombinase polymerase amplification (RPA), selective strand displacement starts with the specific discrimination of SNV and triggers subsequent RPA reaction, releasing the displaced strands to contribute more D-loop structures for the strand-displacement probes to hybridize with the template strands in next amplification cycle. The limitations of current RPA SNV assays regarding specificity and sensitivity have been overcome in this method, as low as 4 pg/μL codon 17 (A>T) mutant genomic DNA (nearly 6 copies) can be accurately determined and robust behavior in clinical specimen analysis was also demonstrated. Moreover, the clinical samples can be analyzed within 35 min from sample extraction to obtaining results. Thus, the SD-triggered RPA strategy provides a pragmatic visualization approach for the rapid, sensitive, and easy detection of codon 17 (A>T) mutation, which is a promising method for point-of-care (POC) SNV assay and exhibits significant potential for future application in clinics.

## 1. Introduction

The single nucleotide variation (SNV) assay has provided substantial assistance in the clinical diagnosis of various genetic diseases, such as β-thalassemia [1], abnormal folate metabolism [2], hereditary hearing impairment [3], and glucose-6-phosphate dehydrogenase deficiency [4]. However, the application of SNV analysis in clinics face great challenges due to the long turnaround time, high testing cost, a shortage of specialized personnel, and limited accessibility to experimental platforms such as real-time polymerase chain reaction (RT-PCR) and next-generation sequencing. The ideal SNV assay, based on point-of-care (POC) requirements, should be capable of rapidly amplifying the target sequence, providing superb single-nucleotide resolution, and producing results that can be easily visualized and interpreted. These would effectively address the current challenges in the popularization of SNV analysis in clinics. Therefore, devising a universally applicable, cost-effective, user-friendly, rapid, and instrument-free approach for the attainment of POC SNV assay and application in clinics is urgently necessary.

In recent times, isothermal amplification has served as a new choice for the detection of SNV, especially recombinase polymerase amplification technology. Recombinase polymerase amplification (RPA) [5] has garnered significant attention from the public owing to its remarkable utility in achieving rapid nucleic acid detection within a mere 20 min and seamless integration with clustered regularly interspaced short palindromic repeats (CRISPR) detection systems [6]. The fast test speed and simple experimental procedure make RPA more easily fulfil POC detection. However, the performance of RPA for mutation detection has a significant drawback on specificity, due to the poor discriminability resulting from the use of long primer and constant temperature

* Corresponding authors.
*E-mail addresses:* 724809959@qq.com (L. Zhang), 13959277591@163.com (Z. Liu), gshee@163.com (Y. Ge).
[1] These authors contributed equally to this work.

https://doi.org/10.1016/j.snb.2023.135075
Received 23 August 2023; Received in revised form 12 November 2023; Accepted 26 November 2023
Available online 29 November 2023

conditions.

In order to overcome the shortcoming of basic RPA on specificity, several measures have been undertaken to enhance the SNV discriminability of RPA, encompassing strategies such as recognition of the mutation base via mismatched primers [7,8], block probes [9], special endonuclease [10] and the CRISPR system [11,12]. But the mismatched primers cannot eliminate background signals and lead false positive results, the block probes weaken the amplification efficiency and hardly shorten the experimental time, special endonuclease and CRISPR system need two-step experimental reaction for SNV assay and increase the complexity of experimental procedures and the risk of aerosol contamination. Therefore, the aforementioned endeavors have been proven insufficiently to meet the clinical demand for a one-step SNV assay possessing ultrasensitivity, high specificity, and rapid test speed.

In search of a viable solution that offers superior specificity compared to mismatched primers and greater efficiency than the employment of block probes, we turned our attention to strand displacement [13], which has been found to differentiate small thermodynamic variations by a difference in a single base, and thereby prompted numerous research undertakings [14]. To identify genotype more specific, the kinetics of strand displacement reaction (SDR) was further explored [15,16] and the specificity of SDR had been continuously optimized [17,18]. In recent years, toehold assisted padlock probe [19] and a unique DNA probe with "Hill-type" cooperativity [20] have been developed and performed good SNV discriminability in toehold-mediated strand displacement processes. Herein, strand displacement possesses superb single-nucleotide resolution in SNV assay.

Thus, in order to endow with the superlative SNV discriminabilty to RPA and achieve rapid reaction in one step, we originally present a novel and universal detection strategy based on strand-displacement-triggered recombinase polymerase amplification (SD-triggered RPA), which integrate the remarkable potential of RPA in rapid testing and the impressive SNV discriminability inherent in SDR. In this study, toehold-mediated strand displacement was firstly integrated into RPA system through an innovative design that toehold and the excessive protector probes co-operated fully to invade the target double-stranded DNA (dsDNA) assisted by the recombinase and contribute to the formation of sufficient D-loop structures for strand-displacement complex to hybridize with the template strands. After SNV discrimination, the concentration of protector probes would increase as SDR working, leading to generate more D-loop structures and promoting the complex binding in next amplification cycle. Then RPA amplification was initiated selectively based on the target genotype, gaining efficient product generation and rapid SNV assay. Additionally, to further realize the POC assay, lateral-flow RPA (LF-RPA) [21] was adopted in this strategy, to meet the current demand for instrument-free result interpretation in clinics (Scheme 1). By selecting codon 17 (A>T) mutation of β-thalassemia as model target variation, as low as 4 pg/μL (nearly 6 copies) of mutant genomic DNA could be accurately determined and robust behavior in 50 cases clinical specimen analysis was also demonstrated by SD-triggered RPA. What's more, the entire experimental process, from sample extraction to obtaining results, could be completed in less than 35 min, indicating a pragmatic strategy for POC SNV assay and huge potential for application in clinics.

## 2. Experimental section

### 2.1. Materials and reagents

All oligonucleotides were synthesized and HPLC-purified by Sangon Biotechnology Co. Ltd. (Zhengzhou, China). The Basic RPA kit and Lateral flow dipsticks were obtained from Suzhou GenDx Biotech Co. Ltd. (Suzhou, China). SYBR Green I was purchased from Solarbio Life Sciences (Beijing, China). All of the sequences are illustrated in Table S1.

### 2.2. Expeditious sample preparation

The peripheral blood samples of thalassemia gene variations were collected at Women and Children's Hospital of Xiamen university. The study was approved by the Ethics Committee of Women and Children's Hospital. And genomic DNA was expeditiously extracted by using the

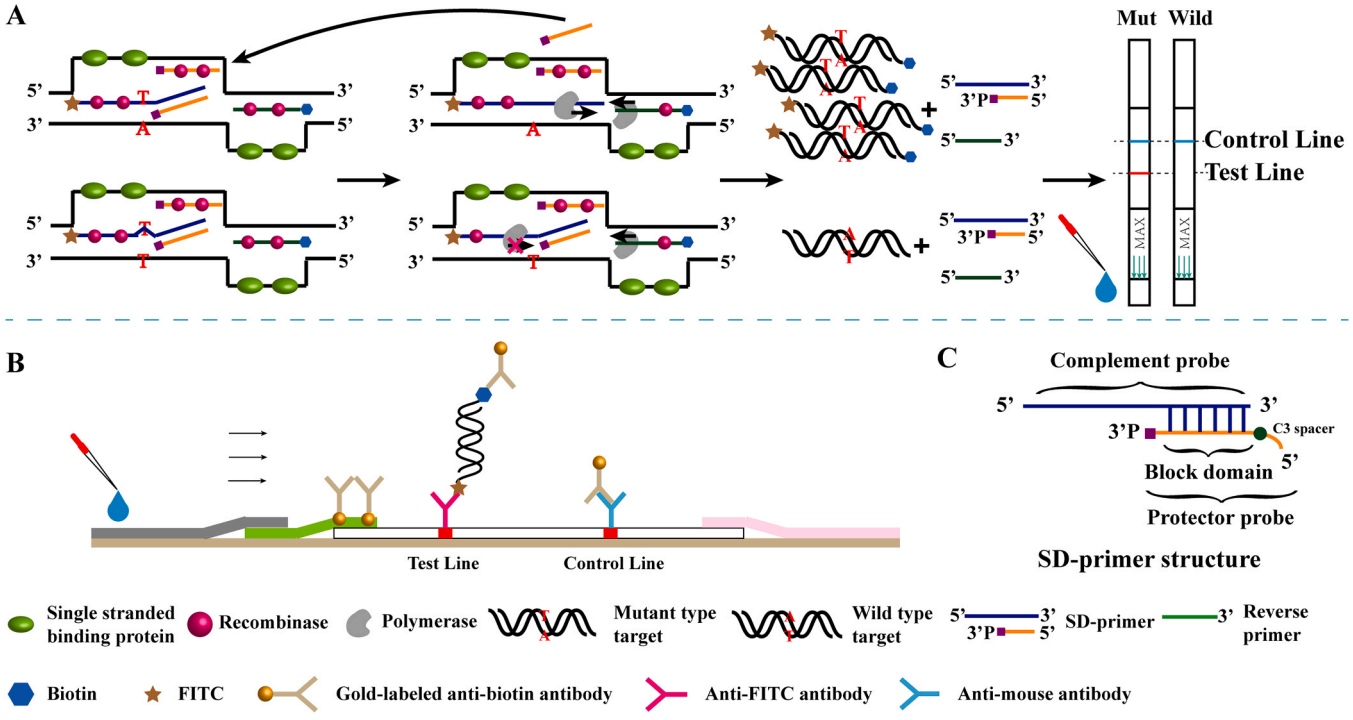


**Scheme 1.** Schematic illustration of the strand-displacement-triggered recombinase polymerase amplification (SD-triggered RPA) for the detection of codon 17 (A>T) mutation.

Nucleic Acid Release System (Tailored Medical Co., Ltd., Shenzhen, China) within a span of 1 min, in strict accordance with the manufacturer's instructions. This process involved two steps, namely the addition of 5 μL of the sample to 25 μL of the lysis solution, followed by an oscillation and instantaneous centrifugation step. Their DNA concentrations were quantified by NanoDrop One Microvolume UV-Vis spectrophotometer (ThermoFisher Scientific, Co., Ltd., Shanghai, China) according to the absorption at 260 nm.

### 2.3. Probe preparation

The probes for SNV discrimination and strand-displacement reaction (named SD-primer below) consisted of a long complement probe to start amplification and a protector probe to inhibit the non-specific amplification of wild-type target. The SD-primer was synthesized at 95 °C for 3 min and 12 °C for 5 min

### 2.4. Real-time RPA reaction

The RPA reaction was performed in 50 μL of a mixture solution containing 14 mM magnesium acetate, 200 nM primer R, 200 nM SD-primer, 1 × rehydration buffer, 1 × SYBR green I, and a certain amount of target DNA. This assay was carried out through real-time PCR at 37 °C for 60 min. Fluorescence signals emitted from SYBR Green I were collected at SYBR channels at the end of every cycle, with each cycle sustained for 1 min

### 2.5. Lateral flow RPA assay

The RPA reaction was performed in 50 μL of a mixture solution containing 14 mM magnesium acetate, 200 nM biotin-labeled primer R, 200 nM FITC-labeled SD-primer, 1 × rehydration buffer and a certain amount of target DNA. The assay was carried out through PCR at 37 °C for different test time (10–60 min). And products were determined with lateral flow dipsticks after a 40-fold dilution in ultrapure water.

### 2.6. Agarose gel electrophoresis

The RPA products were analyzed with 5% agarose gel electrophoresis (AGE) in 0.5 ×TBE buffer (4.5 mM Tris–HCl, pH 7.9, 4.5 mM boric acid, 0.2 mM ethylene diamine tetra acetic acid) at 110 V for 20 min at room temperature. The results were visualized by a Tanon-2500 Imaging System (Tanon Co., Ltd., Shanghai, China).

## 3. Results and discussion

### 3.1. Principle of SD-triggered RPA

Codon 17 (A>T) mutation, the most common SNV of β-thalassemia, was selected as model target variation to test and verify the performance of the proposed method. The principle of SD-triggered RPA is schematically shown in Scheme 1. In SD-triggered RPA, reverse primers were modified with biotin and SD-primers serving as forward primers were generated through a hybridization process between a FITC-labeled complement probe and a protector probe (Scheme 1C). At the initial stage, recombinase bind the excessive protector probes and the toehold of SD-primers respectively to form a nucleoprotein filament, two types of the recombinase-primer complexes can search for target homologous sequences in dsDNA. Once the target sequences is located, two types of the complexes invade the dsDNA and form a D-loop structures respectively. In D-loop structure, one side of the D-loop is double-stranded where the primer hybridizes with the template strand, initiating a strand exchange reaction, whereas the other side of the D-loop remains single-stranded the unwound complementary strand that is stabilized by the single stranded binding (SSB) proteins. In this principle, the D-loop structures caused from the recombinase- protector probes complexes skillfully provide the sufficient space for strand-displacement reaction in subsequent reactions. When mutant targets are present, strand-displacement reaction is initiated following the identification of the specific mutant base, and releasing the single-strand protector probes in a recurring manner, which contributed to providing adequate D-loop structures at the next amplification cycle with cooperation of recombinase. Finally, RPA is triggered along with the strand-displacement reaction running and DNA polymerase initiate the synthesis from the free 3′-OH at the end of the primers, producing a large number of dsDNA products labeled with biotin at 5′ end and FITC at another 5′ end. But when wild-type targets were present, one-base mismatch in the toehold region that closest to the protector probe would leave off the SDR and prevent the SD-triggered RPA, resulting in no products generation (Scheme 1A).

The principle of the lateral flow system for result read-out was shown in Scheme 1B. Upon the amplification products pass through the conjugation pad, biotin modified at the 5′ end of the products undergone conjugation with gold-labelled anti-biotin antibodies, thereby instigating the formation of product-antibody immune complexes. Then the generated FITC-labelled immune complexes were captured by anti-FITC antibodies, generating positive signals at the test line. Excess anti-biotin antibodies conjugated with gold nanoparticles were trapped by anti-mouse antibodies immobilized on the control line. The genotype of the target was deemed to be mutant type only when both the test line and control line manifest clear red bands. In contrast, if solely the control line appears as a visible red band, the genotype of the target was wild type.

### 3.2. Feasibility of SD-triggered RPA

To evaluate the feasibility of SD-triggered RPA, the synthesized mutant targets and the wild-type targets were detected and analyzed by 4% agarose gel electrophoresis (Fig. 1A), real-time fluorescence curve (Fig. 1B) and lateral flow strips (Fig. 1C). As shown in Fig. 1A, RPA products were observed in the basic RPA reaction for both mutant and wild-type target genotypes. The amplification products of wild-type targets demonstrated an obvious band in gel, which was lighter than that obtained from the mutant-type products. This indicated that the basic RPA lacked sufficient specificity for mutation discrimination. But when SD-triggered RPA technology was employed, the products band was still prominent in mutant targets detection, the amplification products of wild-type targets were almost invisible in corresponding lane.

In fluorescence assay (Fig. 1B), the fluorescence signals increased when both genotypes were detected by basic RPA. However, the significant improvements in SNV discriminability were observed as SD-triggered RPA was carried out. The amplification curves obtained from mutant-type and wild-type targets differed distinctly from each other. Furthermore, no non-specific signal increased during wild-type targets analysis, revealing that the innovative design of introducing SDR into RPA was able to substantially enhance the discriminability for SNV assay. The results gained from the strips also supported the novelty of our strategy (Fig. 1C). Moreover, by utilizing the developed principle, the genotype of target DNA can be accurately identified using different analytical platforms such as agarose gel electrophoresis, real-time fluorescence assays, and lateral flow technology. These provide compelling evidences for the feasibility of SD-triggered RPA and its superiority compared to basic RPA.

### 3.3. Optimization of the SD-triggered RPA strategy

In our research, SNV discriminability derived from the combination of the free energy change caused from mismatched base in the toehold region and the blocking performance stemmed from the competitive displacement between SD-primer and template. To acquire the optimal SD-triggered RPA reaction with higher specificity and efficiency, the

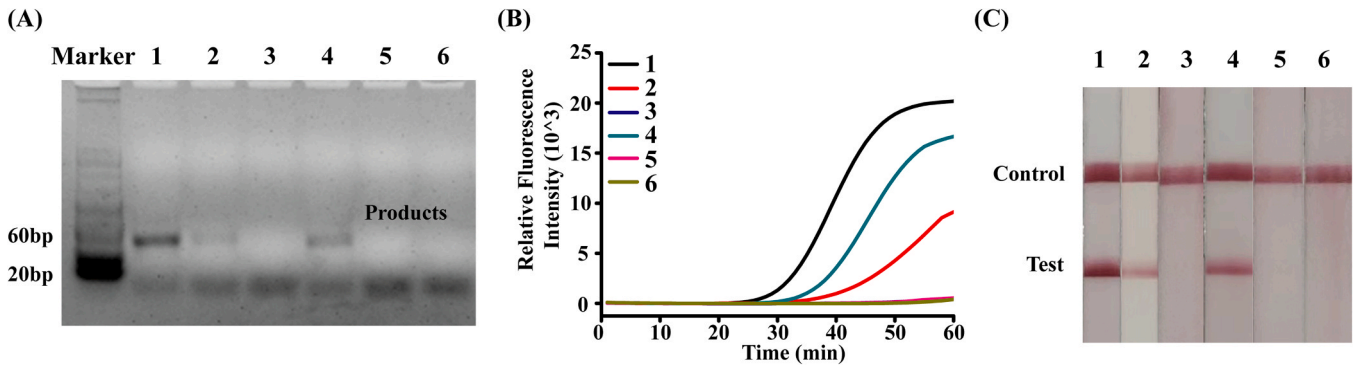


**Fig. 1.** The feasibility verification of basic RPA (1−3) and proposed strategy (4−6) by real-time agarose gel electrophoresis (A), fluorescence analysis (B), and lateral flow assay (C) to detect the mutant targets (1, 4), wild-type targets (2, 5) and blank controls (3, 6).

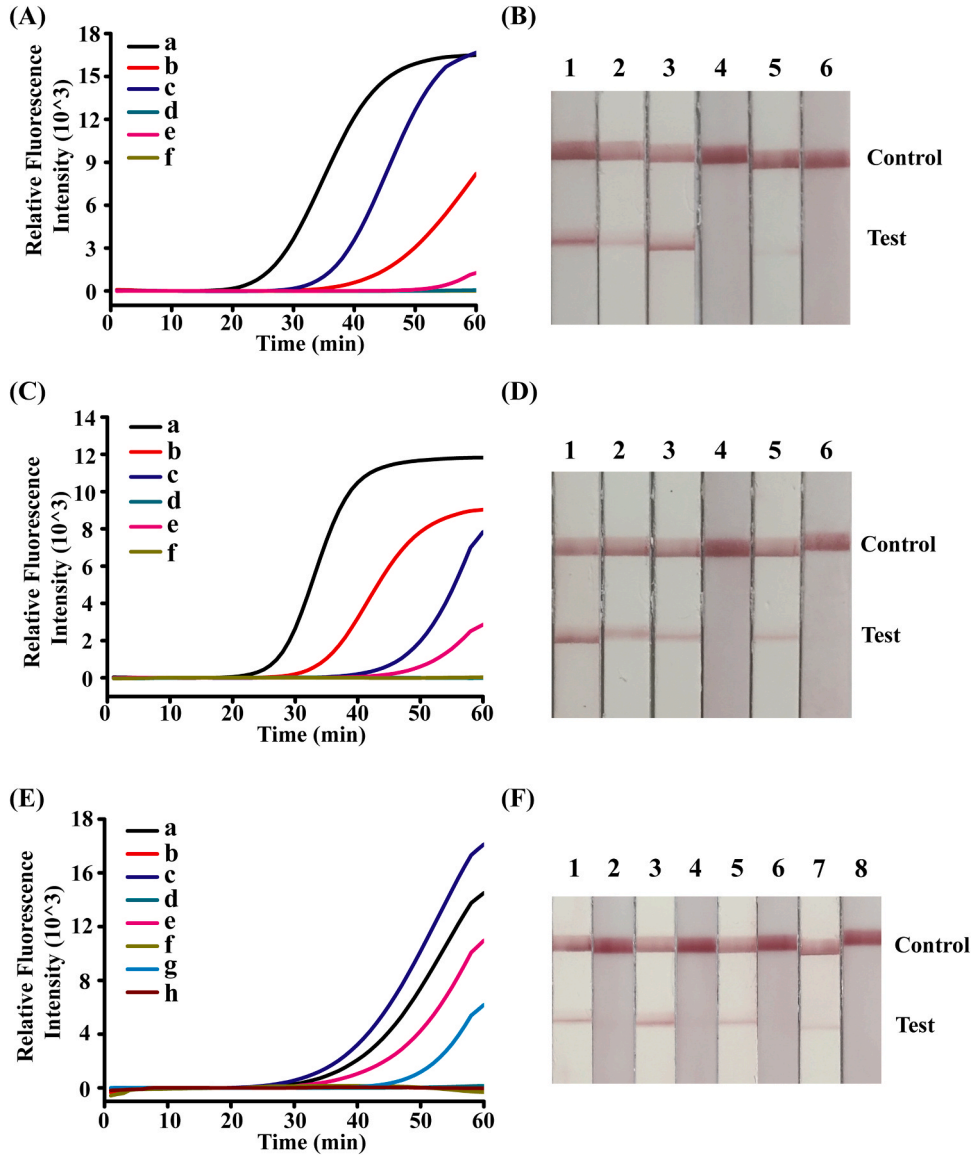


**Fig. 2.** (A) The fluorescence analysis of the SD-triggered RPA strategy to detect mutant (a, c, e) and wild type (b, d, f) target with 8 bp (a, b), 9 bp (c, d), 10 bp (e, f) of the block domain length. (B) The lateral flow assay of the SD-triggered RPA strategy to detect mutant (1, 3, 5) and wild type (2, 4, 6) target with 8 bp (1, 2), 9 bp (3, 4), 10 bp (5, 6) of the block domain length. (C) The fluorescence analysis of the SD-triggered RPA strategy to detect mutant (a, c, e) and wild type (b, d, f) target with 17 nt (a, b), 15 nt (c, d), 13 nt (e, f) of the toehold length. (D) The lateral flow assay of the SD-triggered RPA strategy to detect mutant (1, 3, 5) and wild type (2, 4, 6) target with 17 nt (1, 2), 15 nt (3, 4), 13 nt (5, 6) of the toehold length. (E) The fluorescence analysis of the SD-triggered RPA strategy to detect mutant (a, c, e) and wild type (b, d, f) target under 35 ℃ (a, b), 37 ℃ (c, d), 39 ℃ (e, f), and 41 ℃ (g, h) of temperature condition. (F) The lateral flow assay of the SD-triggered RPA strategy to detect mutant (1, 3, 5, 7) and wild type (2, 4, 6, 8) target under 35 ℃ (1, 2), 37 ℃ (3, 4), 39 ℃ (5, 6), and 41 ℃ (7, 8) of temperature condition.

reaction temperature, the number of bases in block domain and the toehold length of SD-primers, were explored in this study.

The choice of block domain length was determined by two main constraints: 1) the minimal length of block domain was restricted by the integrity/stability of the double-stranded structure formed between the complement probe and the protector probe at reaction temperature; and 2) the longer block domain the slower reaction rate of SDR, and the higher melting temperature of the complementary region [17]; The longer the structure of the block domain, the more stable it would be, making it more difficult for the protector probes to be displaced by the template. This results in better blocking performance. In order to single out the most suitable length of block domain which exhibit great blocking performance and have minimal adverse effects on the efficiency of the assay, in our study, the block domain consisting of 8, 9, or 10 base pairs was firstly evaluated. As shown in Fig. 2 A, when the block domain consisted of 8 base pairs, the positive results were generated in detecting both mutant-type and wild-type targets by fluorescence assay. This suggested that the block domain of 8 base pairs cannot form a sufficiently stable SD-primer structure for mutation discrimination, resulting in the generation of background signals. When the number of bases in block domain increased to 10, although the background signals of the wild-type targets were eliminated, the positive signals of the mutant-type targets were also substantially suppressed, because the formed structure in SD-primer was too stable to initiate the strand displacement reaction. When the length of the block domain was 9 bases, the best performance occurred that the two genotypes had a high degree of differentiation with almost no background signal, indicating that 9 bases was the optimal length of block domain for SNV assay. The test results obtained from lateral flow strips also agreed with the optimization by fluorescence assay (Fig. 2B).

The independent strand-displacement reaction (SDR) is reversible reaction, and toeholds provide a means to increase the rate of strand displacement by increasing the attempt frequency for three-way branch migration. The ratio of the rate of the forward and reverse reaction is given by

$$\sqrt{\mathrm{K}f/\mathrm{K}r} = \mathrm{e}^{-\Delta G^{\circ}/2RT}$$

where K*f* is the rate constant for forward reaction and K*r* is the corresponding rate constant for the reverse reaction, and ΔG° is the standard free energy of hybridization of target with toehold. As ΔG° becomes more negative for longer toeholds, the equilibrium is pushed more strongly toward the forward reaction [22]. Therefore, the toehold length can directly determine the rate of SDR and further determine the efficiency of the SD-triggered RPA. In order to recognize the SNV specifically, the free energy change caused from mutant base in the toehold region should be strong enough compared with ΔG° to serve as a logical gate to change the equilibrium. As shown in Fig. 2 C, when the toehold length was 17 nt, the free energy change caused from mutant base in the toehold region was too low compared with ΔG° to change the equilibrium, leading to a very limited ability to make a distinction between the mutant genotype and the wild-type genotype. When the toehold length was 15 nt and 13 nt, the free energy change became stronger compared with ΔG° and changed the equilibrium, making more effective genotype differentiation in the reaction. Because the toehold length of 15 nt can bring the better amplification efficiency in our strategy, 15-nt toehold length was chosen as the most suitable toehold length of SD-primer. The lateral flow strips also presented the same results as fluorescence assay (Fig. 2D).

Previous research have shown that a temperature increase facilitates the strand displacement reaction [17]. On the other hand, the recommended RPA reaction temperature is between 37 °C and 42 °C, temperatures that are too high or too low would affect the activities of the enzymes in the RPA system. Therefore, to further increase the efficiency in our research with satisfactory specificity, we tested different reaction temperatures for picking out the best running condition (Fig. 2E). As illustrated in Fig. 2E, under the condition of different reaction temperature ranging from 35 ℃ to 41 ℃, the best performance was shown in 37 ℃ system, indicating that 37 ℃ was the most suitable temperature for strand-displacement reaction and RPA system working in our principle design. And others temperature could not excite the maximum efficiency for targets discrimination and amplification, possibly resulted from the decrease of affinity for strand hybridization and the weakened enzymatic activity in RPA system. Consistent results were also obtained from the lateral flow assay (Fig. 2 F).

### 3.4. Performance analysis of the proposed strategy

After enhancing the performance of the proposed strategy by optimizing experimental conditions and screening the optimal structural design of SD-primers, we evaluated the performance of SD-triggered RPA through the detection of targets with varying concentrations of mutant genomic DNA. Within the scope of this research, varying concentrations of mutant genomic DNA ranging from 4 pg/μL to 2 ng/μL were evaluated via fluorescence and lateral flow assays. As negative mimetic samples, wild-type genomic DNA at a concentration of 2 ng/μL was included in the analysis system. To quantify the mutant targets, we defined Rt value as the time when the fluorescence signal raises above the threshold.

As depicted in Fig. 3 A and Fig. 3 C, a clear distinction could be observed between the detection of wild-type and mutant genomic DNA. Furthermore, mimetic samples containing wild-type targets at a concentration of 2 ng/μL failed to generate positive results, thus confirming the remarkable specificity of this approach. In our research, the detection of mutant genomic DNA could be achieved at concentrations as low as 4 pg/μL (equivalent to almost 6 copies), elucidating the high sensitivity of this strategy. The $R_t$ value demonstrated excellent linearity across different target concentrations ranging from 4 pg/μL to 2 ng/μL (Fig. 3B), with a limit of detection of 0.56 pg/μL codon 17 (A>T) mutant genomic DNA in total 60 min analysis. Moreover, the detection of mutant genomic DNA could be accomplished in just 20 min at a target concentration of 20 pg/μL, which is lower than the experimental concentration obtained via routine DNA extraction (Fig. 3D). This suggested the impressive test speed of our strategy, and further elaboration regarding the test speed of our method was presented in Fig. S2. As illustrated in Fig. S3, our methodology demonstrated remarkable discriminability, as it effectively differentiated the codon 17 (A>T) mutation from other SNVs associated with genetic diseases. The above-mentioned results proved that the proposed strategy not only demonstrates remarkable sensitivity and specificity in detecting codon 17 (A>T) mutations, but also exhibited an impressive test speed when compared to current clinical methods (> 4 h). Notably, this strategy does not require specialized instrumentation or complicated procedures, and it could be easily carried out with simple operation, naked-eye result judgement, short turnaround time and under room temperature condition.

### 3.5. Detection of the codon 17 (A>T) mutation in real clinical samples

In order to further investigate the clinical applicability of the proposed methodology, we analyzed 50 clinical samples consisting of 25 β-thalassemia samples with codon 17 (A>T) mutations and 25 healthy human samples via SD-triggered RPA. According to the performance of the strategy in varying test durations, we selected the test duration of 30 min for clinical samples analysis, as the products band could be adequately recognizable in this test duration (Fig. 3D). Subsequently, we compared the detection outcomes obtained from SD-triggered RPA against those derived from the clinical combined approach of PCR and reverse cross-blot hybridization.

The test results and detailed information of 50 cases of clinical specimens were demonstrated in Table 1, and the results obtained from lateral flow strips of all samples were shown in Fig. S4. Utilizing the

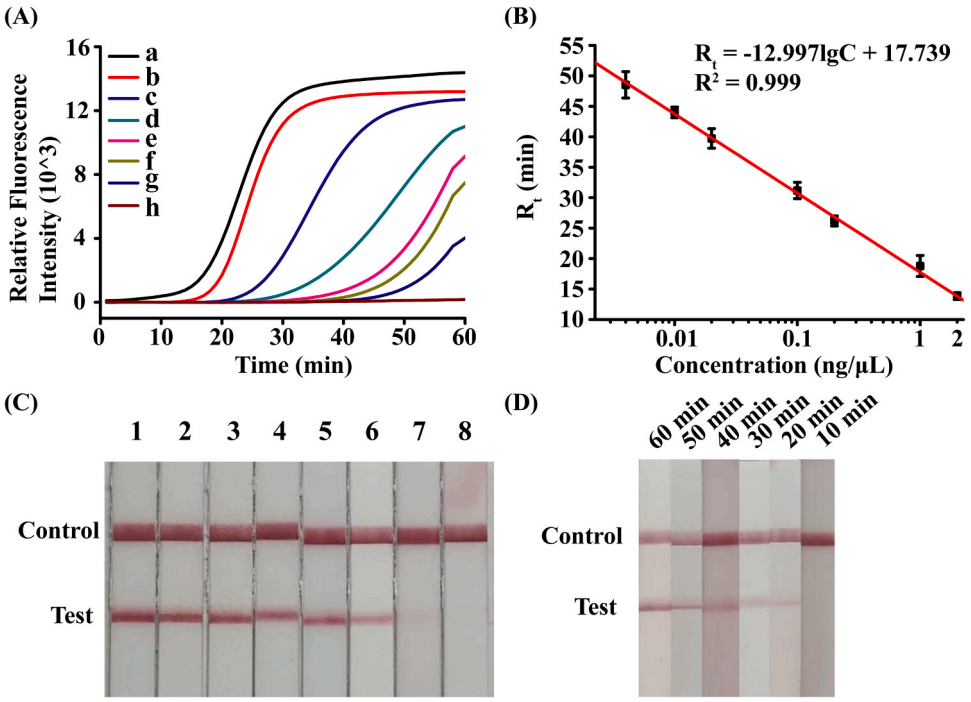


**Fig. 3.** (A) Real-time fluorescence curves of 2 ng/μL, 1 ng/μL, 200 pg/μL, 100 pg/μL, 20 pg/μL, 10 pg/μL, 4 pg/μL codon 17 (A>T) mutant genomic DNA (curve a to g) by SD-triggered RPA, as well as 2 ng/μL wild-type genomic DNA (curve h). (B) The calibration curve of Rt constructed by plotting different concentrations of mutant genomic DNA, with the error bars indicating the standard deviation derived from three replicated experiments. (C) Lateral flow assays of 2 ng/μL, 1 ng/μL, 200 pg/μL, 100 pg/μL, 20 pg/μL, 10 pg/μL, 4 pg/μL codon 17 (A>T) mutant genomic DNA (lane 1–7) and 2 ng/μL wild-type genomic DNA (lane 8) by SD-triggered RPA. (D) Lateral flow assays performed on 20 pg/μL codon 17 (A>T) mutant genomic DNA for varying test durations, ranging from 10 to 60 min.

**Table 1**
Comparison of our proposed assay and the clinical combined approach of PCR and reverse cross-blot hybridization for detecting codon 17 (A>T) mutation in real clinical specimens.

| Method | | Mutant type | Wild type | Sensitivity | Specificity | PPV | NPV |
|---|---|---|---|---|---|---|---|
| **SD-triggerd RPA** | **Positive** | **25** | **0** | **100%** | **100%** | **100%** | **100%** |
| | **Negative** | **0** | **25** | | | | |
| **Clinical method** | **Positive** | **25** | **0** | **100%** | **100%** | **100%** | **100%** |
| | **Negative** | **0** | **25** | | | | |

proposed methodology, all 25 cases of β-thalassemia samples were identified as codon 17 (A>T) mutations, whereas 25 negative results were obtained from the 25 healthy human samples. These findings indicated a 100% sensitivity and specificity for our strategy, and the 100% precision was also verified additionally (Fig S5). Importantly, the results were exactly consistent with those acquired through clinical combined approach using PCR and reverse cross-blot hybridization (Table S2). This strongly demonstrated the high accuracy and practicality of the proposed strategy for detecting codon 17 (A>T) mutations in clinical samples. Furthermore, it is worth mentioning that the experiment cost is lower than 10 dollars per sample and the entire experimental process can be completed in less than 35 min, including one minute for DNA extraction and 30 min for analysis, representing a significant advancement compared to current methods.

## 4. Conclusion

The present study has successfully developed a lateral flow-based SD-triggered RPA assay for detecting β-thalassemia-related SNV (codon 17 (A>T) mutations). Through the innovative integration of SDR into the RPA system, the defect of current RPA SNV assays regarding specificity or sensitivity have been effectively addressed. In this strategy, we have successfully achieved ultrasensitive detection of 4 pg/μL (equivalent to nearly 6 copies) of mutation genomic DNA through a one-step reaction, exhibiting exceptional single-nucleotide resolution. Moreover, real clinical samples can be accurately detected within 35 min from extraction to results, and the results can be visually judged by lateral flow assays. In general, this novel strategy has distinct advantages including low cost, simple operation, rapid detection, and instrument-free result interpretation, demonstrating the huge potential for point-of-care SNV detection and application in clinics.

## CRediT authorship contribution statement

**Lutan Zhang:** Methodology, Investigation, Writing – original draft. **Lulu Xu:** Writing – review & editing, Validation. **Jian Zhang:** Project administration. **Wenbo Wang:** Formal analysis. **Yanru Huang:** Data curation. **Yixi Zhou:** Project administration. **Xingmei Yao:** Visualization. **Zhaohui Liu:** Supervision. **Yunsheng Ge:** Conceptualization, Resources.

## Declaration of Competing Interest

The authors declare that they have no known competing financial interests or personal relationships that could have appeared to influence the work reported in this paper.

## Data availability

No data was used for the research described in the article.

## Acknowledgements

This work was sponsored by the Medical and Health Guidance Project of Xiamen (3502Z20209196), Fujian Provincial Health Technology Project (2022QNB023), Natural Science Foundation of Fujian Province (2023J011608), Natural Science Foundation of Shandong Province (ZR2022QH034), Natural Science Foundation of Fujian Province (2021J011352).

## Appendix A. Supporting information

Supplementary data associated with this article can be found in the online version at doi:10.1016/j.snb.2023.135075.

## References

[1] T. Munkongdee, P. Chen, P. Winichagoon, S. Fucharoen, K. Paiboonsukwong, Update in laboratory diagnosis of thalassemia, Front. Mol. Biosci. 7 (2020) 74.
[2] N. Padmanabhan, K. Menelaou, J. Gao, A. Anderson, G.E.T. Blake, T. Li, B.N. Daw, E.D. Watson, Abnormal folate metabolism causes age-, sex- and parent-of-origin-specific haematological defects in mice, J. Physiol. 596 (2018) 4341–4360.
[3] C. Guo, S.S. Huang, Y.Y. Yuan, Y. Zhou, N. Wang, D.Y. Kang, S.Y. Yang, X. Zhang, X. Gao, P. Dai, Hearing Phenotypes of Patients with Hearing Loss Homozygous for the GJB2c.235delc Mutation, Neural Plast. (2020), 8841522.
[4] L. Luzzatto, M. Ally, R. Notaro, Glucose-6-phosphate dehydrogenase deficiency, Blood 136 (2020) 1225–1240.
[5] D.S. Mota, J.M. Guimarães, A.M.D. Gandarilla, J. Filho, W.R. Brito, L.A. M. Mariúba, Recombinase polymerase amplification in the molecular diagnosis of microbiological targets and its applications, Can. J. Microbiol. 68 (2022) 383–402.
[6] W.S. Zhang, J. Pan, F. Li, M. Zhu, M. Xu, H. Zhu, Y. Yu, G. Su, Reverse Transcription Recombinase Polymerase Amplification Coupled with CRISPR-Cas12a for Facile and Highly Sensitive Colorimetric SARS-CoV-2 Detection, Anal. Chem. 93 (2021) 4126–4133.
[7] B.Y.C. Ng, E.J.H. Wee, K. Woods, W. Anderson, F. Antaw, H.Z.H. Tsang, N.P. West, M. Trau, Isothermal Point Mutation Detection: Toward a First-Pass Screening Strategy for Multidrug-Resistant Tuberculosis, Anal. Chem. 89 (2017) 9017–9022.
[8] M.E. Natoli, M.M. Chang, K.A. Kundrod, J.B. Coole, G.E. Airewele, V.N. Tubman, R. R. Richards-Kortum, Allele-specific recombinase polymerase amplification to detect sickle cell disease in low-resource settings, Anal. Chem. 93 (2021) 4832–4840.
[9] L. Zhang, J. Peng, J. Chen, L. Xu, Y. Zhang, Y. Li, J. Zhao, L. Xiang, Y. Ge, W. Cheng, Highly Sensitive Detection of Low-Abundance BRAF V600E Mutation in Fine-Needle Aspiration Samples by Zip Recombinase Polymerase Amplification, Anal. Chem. 93 (2021) 5621–5628.
[10] Y. Ma, H. Wu, S. Chen, C. Xie, J. Hu, X. Qi, X. Ma, Y. Chu, J. Shan, Y. Lu, L. Cui, B. Zou, G. Zhou, FEN1-aided recombinase polymerase amplification (FARPA) for one-pot and multiplex detection of nucleic acids with an ultra-high specificity and sensitivity, Biosens. Bioelectron. 237 (2023), 115456.
[11] P. Liu, X. Wang, J. Liang, Q. Dong, J. Zhang, D. Liu, S. Wang, J. Bi, W. Liu, Z. Wang, L. Chen, L. Liu, X. Huang, G. Zhang, A. Recombinase, Polymerase Amplification-Coupled Cas12a Mutant-Based Module for Efficient Detection of Streptomycin-Resistant Mutations in Mycobacterium tuberculosis, Front. Microbiol. 12 (2021), 796916.
[12] H. Liu, J. Wang, X. Hu, X. Tang, C. Zhang, A rapid and high-throughput Helicobacter pylori RPA-CRISPR/Cas12a-based nucleic acid detection system, Clin. Chim. Acta 540 (2023), 117201.
[13] D.Y. Zhang, G. Seelig, Dynamic DNA nanotechnology using strand-displacement reactions, Nat. Chem. 3 (2011) 103–113.
[14] Z. Zhang, D. Zeng, H. Ma, G. Feng, J. Hu, L. He, C. Li, C. Fan, A DNA-Origami chip platform for label-free SNP genotyping using toehold-mediated strand displacement, Small 6 (2010) 1854–1858.
[15] P. Irmisch, T.E. Ouldridge, R. Seidel, Modeling DNA-Strand Displacement Reactions in the Presence of Base-Pair Mismatches, J. Am. Chem. Soc. 142 (2020) 11451–11463.
[16] R.R. Machinek, T.E. Ouldridge, N.E. Haley, J. Bath, A.J. Turberfield, Programmable energy landscapes for kinetic control of DNA strand displacement, Nat. Commun. 5 (2014) 5324.
[17] D.A. Khodakov, A.S. Khodakova, D.M. Huang, A. Linacre, A.V. Ellis, Protected DNA strand displacement for enhanced single nucleotide discrimination in double-stranded DNA, Sci. Rep. 5 (2015) 8721.
[18] D.Y. Zhang, S.X. Chen, P. Yin, Optimizing the specificity of nucleic acid hybridization, Nat. Chem. 4 (2012) 208–214.
[19] Y. Gao, H. Qiao, V. Pan, Z. Wang, J. Li, Y. Wei, Y. Ke, H. Qi, Accurate genotyping of fragmented DNA using a toehold assisted padlock probe, Biosens. Bioelectron. 179 (2021), 113079.
[20] H. Hao, Y. Li, B. Yang, S. Lou, Z. Guo, W. Lu, Simulation-Guided Rational Design of DNA Probe for Accurate Discrimination of Single-Nucleotide Variants Based on "Hill-Type" Cooperativity, Anal. Chem. 95 (2023) 2893–2900.
[21] D. Liu, H. Shen, Y. Zhang, D. Shen, M. Zhu, Y. Song, Z. Zhu, C. Yang, A microfluidic-integrated lateral flow recombinase polymerase amplification (MI-IF-RPA) assay for rapid COVID-19 detection, Lab. Chip. 21 (2021) 2019–2026.
[22] F. Simmel, B. Yurke, H. Singh, Principles and applications of nucleic acid strand displacement reactions, Chem. Rev. 119 (2019) 6326–6369.

**Lutan Zhang** is currently a professor of The Department of Central Laboratory, The Women and Children's Hospital Affiliated to Xiamen University. His research interest is the development of biosensing strategy for clinical diagnosis.

**Lulu Xu** is currently an associate professor of Shandong Provincial Hospital Affiliated to Shandong First Medical University majoring in clinical laboratory diagnosis. Her research interest is the development of biosensing strategy for clinical laboratory diagnosis.

**Jian Zhang** is currently a research assistant of The Women and Children's Hospital Affiliated to Xiamen University majoring in clinical laboratory diagnosis. Her research interest is the development of biosensing strategy for clinical diagnosis.

**Wenbo Wang** is currently a technicist of The Women and Children's Hospital Affiliated to Xiamen University. Her research interest is the development of biosensing strategy for clinical diagnosis.

**Yanru Huang** is currently a technicist of The Women and Children's Hospital Affiliated to Xiamen University. Her research interest is the development of biosensing strategy for clinical diagnosis.

**Yixi Zhou** is currently a technicist of The Women and Children's Hospital Affiliated to Xiamen University. His research interest is the development of biosensing strategy for clinical diagnosis.

**Xinmei Yao** is currently a technicist of The Women and Children's Hospital Affiliated to Xiamen University. Her research interest is the development of biosensing strategy for clinical diagnosis.

**Zhaohui Liu** is currently a professor of The Graduate School of Fujian Medical University. His research interest is the development of biosensing strategy for clinical laboratory diagnosis.

**Yunsheng Ge** is currently a professor in The Department of Central Laboratory, The Women and Children's Hospital Affiliated to Xiamen University. His research interest is the development of biosensing strategy for clinical laboratory diagnosis.